JACS Au
AN OPEN ACCESS JOURNAL OF THE AMERICAN CHEMICAL SOCIETY

pubs.acs.org/jacsau
Perspective

DNA Nanotags for Multiplexed Single-Particle Electron Microscopy and *In Situ* Electron Cryotomography

Published as part of JACS Au special issue "DNA Nanotechnology for Optoelectronics and Biomedicine".

Yuanfang Chen,[#] Yiqian Huang,[#] and Yuhe R. Yang*

Cite This: *JACS Au* 2025, 5, 17−27

ABSTRACT: DNA nanostructures present new opportunities as Nanotags for electron microscopy (EM) imaging, leveraging their high programmability, unique shapes, biomolecule conjugation capability, and stability compatible with standard cryogenic sample preparation protocols. This perspective highlights the potential of DNA Nanotags to enable high-throughput multiplexed EM analysis and facilitate *in situ* particle identification for cryogenic electron tomography (cryo-ET). Meanwhile, applying Nanotags in live-cell environments requires the efficient cellular uptake of intact structures and successful cytosolic migration. Promising strategies such as employing direct cytosolic delivery platforms and expressing RNA-based Nanotags *in situ* are discussed, while more systematic studies are needed to fully understand the intracellular trafficking and achieve precise localization of DNA Nanotags.

KEYWORDS: *DNA nanostructures, nanotags, electron microscopy, cryo-electron tomography*

INTRODUCTION

Cryo-electron microscopy (cryo-EM) has emerged as a formidable technique in determining the three-dimensional (3D) structures of biomacromolecules at near-atomic resolution.[1] However, this powerful technology faces significant throughput limitations: each sample requires a unique grid, and data acquisition for individual cryo-EM grids is time-intensive, often spanning several hours or even days.[2] Enabling the concurrent characterization of mixed particle species on a single grid holds a good chance to accelerate the research and development (R&D) cycle of new pharmaceuticals. For example, one could simultaneous analysis of multiple drugs against G protein-coupled receptors (GPCRs) and their binding pockets,[3,4] as well as one specific drug ligand against GPCRome-wide targets, particularly understudied and orphan receptors. This type of multiplexed imaging offers structural insights toward functional selectivity and signaling bias of each drug molecule to impart activations in distinct pathways.[5] Although a prototype instrument was developed to dispense each individual gold nanoparticle sample from a 96-well plate to defined locations on a TEM grid using a piezoelectric capillary dispensing system,[6] the time required to dispense multiple specimens (∼4 h for delivering 96 spots) is incompatible with cryo-EM grid preparation of biological samples.[7−10] To date, achieving high-throughput multiplexed cryo-EM imaging remains challenging.

Moving forward, *in situ* characterization requires the identification of targets within a native cellular environment crowded with cytoskeletons, cytoplasmic inclusions, organelles, etc.[11] This complexity poses an even greater challenge concerning target localization. To address these challenges, strategies have been developed to localize targets among intercellular milieu and noises by tagging proteins of interest (POIs) with detectable tags.[12] Current strategies can be categorized into density tags and size tags. Electron microscope (EM)-visible heavy atoms such as gold[13−15] or iron[16−18] can be attached to, and localize target proteins via immunolabeling or genetically encoded metallothionein or ferritin, while iron-rich media required for ferritin-tagging is often toxic to living cells. Nevertheless, the strongly scattered electrons by metal atoms may give a risk of obscuring biological samples during tomography reconstruction.[19] On the other hand, size tags use proteins with adequate sizes for visual detection in EM imaging. For example, an iron-free FerriTag enables nanoscale mapping of Hip1R distribution surrounding clathrin-coated

Received: October 18, 2024
Revised: December 17, 2024
Accepted: December 17, 2024
Published: December 27, 2024

https://doi.org/10.1021/jacsau.4c00986
JACS Au 2025, 5, 17−27

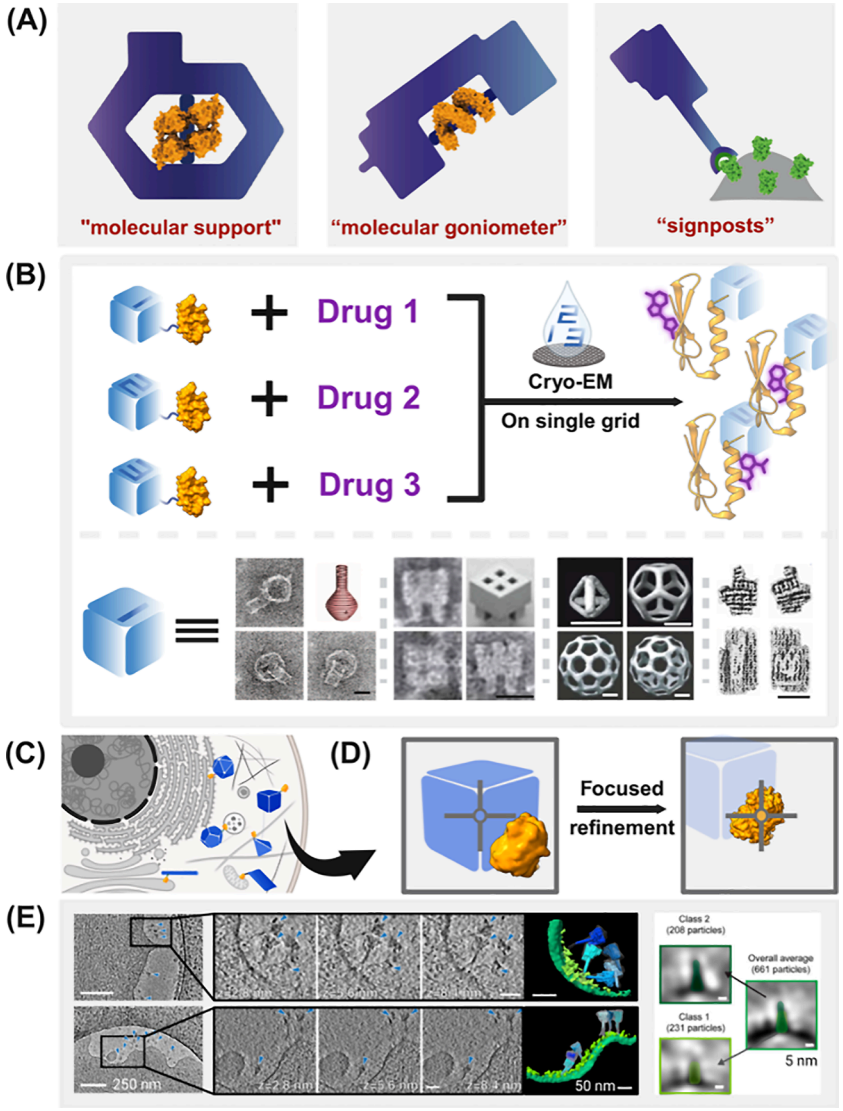

Figure 1. Application of DNA Nanotags to cryo-EM and cryo-ET. (A) "Molecular support" (left) and "molecular goniometer" (middle) rotate DNA binding proteins for cryo-EM reconstruction. DNA origami "signposts" for cellular membrane tagging (right). (B) Conceptual workflow of high throughput cryo-EM-based drug screening using DNA Nanotags (top). Representative structures with distinctive features[28,34,36,75] (bottom). Scale bar: 20 nm. The first panel is reproduced with permission from ref 34. Copyright 2011 American Association for the Advancement of Science. The second panel is reproduced with permission from ref 36. Copyright 2012 American Association for the Advancement of Science. The third panel is reproduced with permission from ref 28. Copyright 2008 Springer Nature. The fourth panel is reproduced from ref 75. Available under a CC-BY license. Copyright 2012 The Authors. (C) Schematic illustration of *in situ* cryo-ET application of DNA Nanotags. The unique shape of Nanotags can localize POIs in a crowded cellular environment. (D) Focused refinement of protein reconstructions. (E) Micrographs and 3D reconstruction results of DNA origami "signposts"-labeled membrane proteins. Reproduced from ref 19. Available under a CC-BY license. Copyright 2021 The Authors.

membrane.[20] The encapsulin-derived genetically encoded multimeric particles (GEMs) with recognizable yet symmetric structural signatures can be exploited to localize particles with precision on the scale of 10−25 nm.[21] Importantly, both iron-free FerriTag and GEM tags can be automatically identified by convolutional neural networks (CNNs). However, neither density tags nor size tags offer asymmetric structures that can precisely pinpoint the location of tagged proteins, instead indicating only a roughly spherical region around the tag. This lack of confident particle picking can result in a high number of invalid false positive particle images, potentially leading to overfitting and model bias during data processing,[22] which hinders reliable structure reconstruction through subtomogram averaging. Here, DNA nanostructure, with its unique and customizable shape, offers a promising approach as novel cryo-electron tomography (cryo-ET) tags, providing precise localization and enhanced visibility.[19]

The field of DNA nanotechnology was first pioneered by Nadrian C. Seeman in the early 1980s, who proposed using DNA to create periodic molecular scaffolds that could crystallize guest molecules.[23,24] By exploiting their programmability, scientists design and assemble DNA molecules into precise and predictable shapes and patterns.[25−28] In 2006, Paul Rothemund introduced the concept of DNA origami,[29] a technique that allows the folding of a long single-stranded DNA (ssDNA) into complex shapes with the help of short staple strands. This strategy enabled the robust creation of

https://doi.org/10.1021/jacsau.4c00986
JACS Au 2025, 5, 17−27

intricate two-dimensional and later three-dimensional nanoscale objects.[30,31]

Several distinct merits empower DNA nanostructures to serve as an effective Nanotag for cryo-EM: (1) The highly distinguishable shapes of DNA nanostructures can serve as unambiguous indicators for other biomolecules under EM. Hundreds of elaborate structures with defined densities,[32] curvatures,[33,34] and even intricate shapes such as Chinese characters[35,36] can be easily created following simple yet robust strategies (Figure 1B, bottom). Through rational design, one can engineer asymmetric objects that display different patterns from different perspectives under transmission electron microscopy (TEM),[32,36] providing valuable information for orientation assignment algorithms. Excitingly, computer-aided methods have emerged to automate the generation of complex DNA origami objects, including DEADLUS,[37] TALOS,[38] DNAxiS,[38] and 4vHelix.[39] (2) DNA nanostructures can be coupled with lipids,[40] peptides[41] and proteins[41] via diverse conjugation methods. It is noteworthy that the conjugation between DNA and proteins does not necessarily depend on genetically fused protein tags. Oligonucleotides are possible to be attached to minimally modified proteins,[41] preserving their natural state. (3) DNA nanostructures can remain structurally intact under sample preparation conditions for most cryo-EM applications. Current research demonstrated that DNA nanostructures can withstand common protein buffers (e.g., tris-buffered saline (TBS)[42] and phosphate-buffered saline (PBS) buffer[43,44]) with the addition of trace stabilizing cations during cryo-EM sample preparation.[45] It can also tolerate some detergents, such as n-Dodecyl-β-D-maltoside (DDM) and lauryl maltose neopentyl glycol (LMNG), that are often indispensable for membrane protein samples (Yang group unpublished results). For *in situ* cryo-ET applications, various modification strategies have been developed, such as lipid bilayer coating,[46] protein coating,[47] polymer coating,[48] and UV welding,[49] that allow DNA nanostructures to endure cell cultivation conditions for at least several hours,[50] which is within the typical time frame for cryogenic sample preparation.[51] Together, the DNA nanostructure meets the primary requirements for use as Nanotags in EM bioimaging. In fact, DNA nanostructures have already been utilized in cryo-EM[52−55] and cryo-ET[19] to assist in the characterization of biological samples (Figure 1A), illustrating their compatibility with structural biology. This Perspective first delves into the critical challenges associated with the application of this emerging DNA Nanotag strategy in multiplexed single-particle cryo-EM imaging. Further, we provide the prospect of using Nanotags within a cellular environment for *in situ* cryo-ET, and discuss the two main technical questions, namely cell-entering of Nanotags and their intracellular trafficking.

MULTIPLEXED SINGLE-PARTICLE EM

DNA nanotechnology was initially proposed as a tool for X-ray structural analysis according to Seeman's pioneering vision.[23] In the following decades, cryo-EM technology emerged and became a mainstream technique in structural biology,[56] when the potential of DNA nanostructures in cryo-EM started to be realized.[52] It has been noticed that the programmable shape of DNA nanostructures can provide priori knowledge, such as orientation angles of target protein, to the single particle analysis (SPA) algorithms.[53,54] However, only DNA-binding proteins can be accurately rotated by these scaffolds. For a more generic purpose, DNA Nanotags can serve as particle identifiers, marking the types of proteins in a mixed sample and offering novel possibilities for the high-throughput screening of protein complexes by multiplexed cryo-EM imaging (Figure 1B, top).

Admittedly, the strong contrast of DNA molecules can cause misalignment of the target protein, and blur the particle averages, as already observed in both negative staining EM (ns-EM)[57−59] and cryo-EM[52,60,61] analysis of DNA nanostructure-protein complexes. Therefore, providing the necessary spacing for POI on Nanotags would be beneficial. For example, Aissaoui et al. reported a V-shaped DNA origami scaffold designed to accommodate POIs, where the proteins are anchored at the center of the "V" by a long double-stranded DNA (dsDNA), effectively isolating them from the framework.[55] Adopting this strategy, an ns-EM data set of RNAP protein (~450 kDa) with approximately 4,000 particles yielded a 25 Å resolution map. Notably, despite its persistence length of ~50 nm,[62] the nonnegligible flexibility of dsDNA[63] cannot be considered as a rigid linker for hybridizing protein and Nanotag. Considering the challengeable cryo-EM reconstruction of multidomain proteins[64] (which are connected by short amino acid sequences[65]), using a flexible dsDNA spacer would likely introduce additional conformational heterogeneity, and consequently compromise the POI resolutions.

Novel data processing methods can be expected to weaken or subtract Nanotag signals in a high-throughput manner after identifying their contextual information (Figure 1D). In recent years, Zhang's group has developed a series of algorithms that can automatically estimate and weaken unwanted signals in macromolecular complexes to improve the alignment reliability of target proteins.[66−68] For example, their approach searched the microtubule networks by multicurve fitting, modeled the tubulin-lattice signals, and then removed them. The removal of the superior tubulin-lattice signal improved the alignment and reconstruction of outer-arm dynein (OAD).[66] With the shape information on predefined DNA nanostructures, these signal removal methods should be readily implementable in Nanotag systems to suppress the DNA signals. Another approach, termed "composite masks",[69] allows for focused refinement of a small region while preserving the low-frequency signals from detergent micelle. They used a tight mask to separate POI from micelle signals, as well as a loose mask to low-pass filter the micelles to reduce noise and overfitting, thereby constraining the global alignment during 3D refinement. This idea can be applied to Nanotag-attached proteins, where the orientation assignment of POI particles is often interdependent with Nanotag scaffolds.

IN SITU PARTICLE PICKING

As an emerging bioimaging technique, cryo-ET allows for the examination of macromolecules and complexes *in situ*, preserving their native states and interactions within the cellular context. In order to determine high-resolution 3D models, hundreds of thousands of particle subvolumes need to be picked from tomograms. Particle picking can be performed manually, or by template-matching methods in which a known (or manually picked) structure serves as a template.[70] Alternatively, template-free methods can extract candidate particles based solely on their size.[71] Nevertheless, picking particles in a crowded cellular landscape remains challenging.[72] On the one hand, the total electron dose used is limited to protect the sample from radiation damage, resulting in a very low signal-to-noise ratio (SNR) for each tilt frame.[73] On the

https://doi.org/10.1021/jacsau.4c00986
JACS Au 2025, 5, 17−27

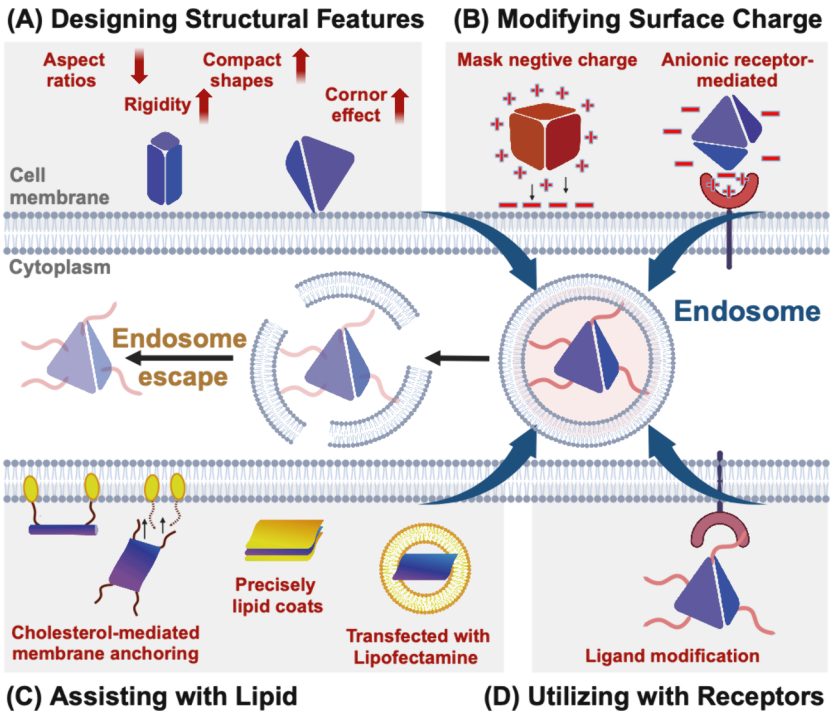

Figure 2. Strategies to improve the efficiency of delivering DNA nanostructures via the endocytosis-lysosome escape pathway.

other hand, macromolecules are densely packed and surrounded by various other structures within cells, making it difficult to identify and isolate individual particles, particularly in low SNR tomograms. Advanced computational approaches based on deep neural network[74] are increasingly employed for the automated picking of large particles with identifiable shapes[21] such as DNA Nanotags.

It has been pointed out that the phosphorus in DNA molecule backbones scatters elastically ∼4× more electrons than the major elements in proteins, such as carbon, oxygen, or nitrogen.[19] DNA Nanotag composed of densely packed DNA molecules may thus generate a stronger contrast in a low SNR tomogram context. Combined with its distinctive shapes, DNA Nanotag holds the potential to provide precise and confident positioning of particles of interest within the crowded and heterogeneous cellular environment (Figure 1C). Based on this idea, the signpost origami tags (SPOTs),[19] which bind to GFP-tagged membrane proteins on the cell surface (Figure 1E, left), shed new light on developing a generally applicable tagging platform for cryo-ET bioimaging. Despite the low-resolution subvolume averaging results of target gB protein, two classes have been obtained that broadly resemble two known conformations of gB (Figure 1E, right), inferring that the presence of SPOTs is compatible with the subvolume alignment and classification process. Encouraged by the extracellular leaflet labeling SPOTs, DNA Nanotags that target cytoplasmic leaflets, organelle membranes, and cytoplasmic biomolecular complexes can be anticipated.

CYTOSOLIC ENTRY OF NANOTAGS

The major challenges in utilizing DNA Nanotags for *in situ* imaging are 2-fold: first, getting them across the cellular membrane into the cytosol; second, enabling intracellular migration to designated subcellular organelles. DNA Nanotags, as nanometric particles, predominantly enter cells via endocytosis.[76] Consequently, numerous strategies have been developed to improve uptake efficiency[47,48,77−95] and promote endosomal escape.[96−99] Alternative approaches focus on direct cytosolic delivery across the cell membrane,[100−104] offering the possibility to better preserve the structural integrity of DNA Nanotags. This procedure necessitates specific modifications to redirect a portion of the Nanotags from primary endocytosis-based pathways.

Strategies to improve the efficiency of delivering DNA nanostructures via the Endocytosis-Lysosome Escape pathway can be categorized into four groups: First, modulating the structural features (Figure 2A). Numerous studies have demonstrated that a higher degree of structural rigidity,[77] compactness,[80] and smaller aspect-ratio[79] are associated with enhanced uptake of bare DNA nanostructures.[78−81] Second, modifying the surface charge (Figure 2B). Coating layers such as oligolysine-PEG,[48] polyethylenimine (PEI),[82] virus capsid,[47] and preadsorbed protein corona[83] can mask the negatively charged DNA backbones, reducing electrostatic repulsion from the plasma membrane. Third, assisting with lipids (Figure 2C). Noncoated DNA nanostructures with single-stranded probes can hybridize with cell-anchored cholesterol-ssDNA, facilitating direct interaction with the cell membrane.[87−89] Alternatively, DNA nanostructures can be coated with cationic lipids via electrostatic interactions[84] or with noncationic lipids through hydrophobic interactions using the Frame-Guided Assembly (FGA) strategy,[85,86] both of which have been shown to enhance cellular uptake. Lastly, receptor targeting (Figure 2D). Reported ligand−receptor pairs can facilitate receptor-mediated endocytic pathways, with ligands such as transferrin,[90] folate,[91,92] aptamers,[93,94] and tumor-penetrating peptide,[95] etc. having been explored.

Next, after DNA Nanotags are initially captured by early lysosomes during endocytosis, endosomal escape is crucial for delivery to the cytosol. Various endosomal escape peptides have been explored,[96] among which hemagglutinin (HA) fusogenic peptide[97] and aurein 1.2[98] are applied to DNA

https://doi.org/10.1021/jacsau.4c00986
JACS Au 2025, 5, 17−27

structures. These peptides can be loaded through chemical conjugation or electrostatic adsorption, with the latter allowing for higher peptide coverage on the nanostructures.[99]

The strategies described above have significantly enhanced the internalization of DNA nanostructures via endocytosis. For instance, transferrin-modified DNA nanostructures have shown an uptake efficiency up to 22-fold higher than the unmodified ones in KB cells.[90] Modifications with HA fusogenic peptide have achieved endosomal escape rates as high as 61%.[97] However, several key points merit attention. First, the cellular uptake of DNA nanostructures significantly depends on the cell types. Generally, immune cells and cancer cells exhibit a higher efficiency of internalization compared to other cells.[79] Second, current experimental approaches applied to assess cellular uptake efficiency typically include fluorescence confocal microscopy, flow cytometry, and quantitative PCR (qPCR). These methods frequently employ DNA nanostructures labeled with single or dual fluorescent dyes to determine spatial localization or through FRET (Förster Resonance Energy Transfer) to evaluate interdye distances and thus infer the structural integrity. However, structural characterization techniques such as transmission electron microscopy (TEM) or atomic force microscopy (AFM) are rarely used to evaluate the structural integrity of DNA nanostructures postcell lysis.

Ideally, for *in situ* EM imaging applications, DNA Nanotags should preserve their intricate structural features upon reaching their intended cellular destinations. Consequently, strategies promoting direct cytosolic uptake, which circumvent endosomal pathways, are of considerable value. These methods prevent DNA Nanotags from exposure to degradative conditions (e.g., low pH) within endo/lysosomes, where significant disintegration can occur.[105] Physical approaches that enable the direct delivery of DNA nanostructures to the cytoplasm include electrotransfection,[100] nanoneedles,[101] and "cell squeezing" technique.[102] Electrotransfection, commonly used for plasmids, requires a spermidine buffer to maintain the structural integrity of DNA nanostructures at high voltages. The latter two methods increase membrane permeability by inducing mechanical stress and creating membrane pores, heavily relying on specialized instruments. In addition, while studies report minimal impact on cell survival, the structural integrity of DNA nanostructures postdelivery remains uncertain. Thiol-mediated[103,106,107] uptake holds promise for cytosolic entry at more native cell states (Figure 3A). Yan et al. developed a DNA nanodevice, CytoDirect, which integrates disulfide moieties and human epidermal growth factor receptor 2 (HER2) affibodies.[103] The HER2 affibody, functioning as a targeting domain, brings the disulfide bonds on the DNA nanodevice into the proximity of the thiol groups on the cell surface. After internalization, intracellular endogenous glutathione (GSH) cleaves these disulfide bonds, enabling the rapid release of the nanodevice from the cell membrane into the cytosol. It is noted that no experimental data regarding the structural integrity of the released nanodevices have been reported.

Although research on the direct cytosolic uptake of DNA nanostructures is limited, recent advancements in mRNA vaccine delivery systems offer valuable insights. Lewis et al. developed a proteolipid vehicle (PLV) that facilitates membrane fusion between PLVs and the cell membrane by incorporating fusion-associated small transmembrane (FAST) proteins[104] (Figure 3B). Due to FAST proteins being compatible across various cell types,[108] PLVs have achieved

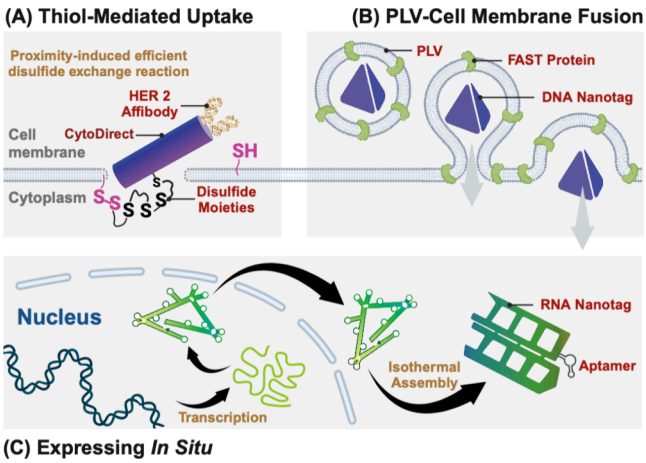

Figure 3. Strategies to direct cytosolic delivery across the cellular membrane or expressing Nanotags *in situ*.

efficient delivery of mRNA and plasmid DNA (pDNA) into different cell lines including AC10, H1299, and HEK293T.[104] The PLV particles, ∼ 80 nm in size, align well with the size range of the DNA nanostructures. Moreover, this delivery mechanism does not necessitate modifications of the DNA nanostructures. These attributes, collectively, establish PLVs as a highly promising platform for the cytosolic entry of DNA Nanotags.

IN SITU EXPRESSION OF NANOTAGS

Expressing Nanotags *in situ* presents another solution to circumvent the difficulties associated with intracellular delivery. Here, structures constructed with only one single-stranded nucleic acid hold the potential to be intracellularly replicated and expressed once the nanostructure-forming "pseudogenes" are transfected (Figure 3C). To fabricate such single-stranded nanostructures with size and shape diversities, universal strategies, termed single-stranded origami (ssOrigami), have emerged.

The key challenge of folding a compact single-stranded structure is to avoid kinetic traps imposed by knots during designing the strand routing.[109] Geary et al. inserted extra 180° kissing loops between each antiparallel double-crossover (DX) to decrease the topological complexity.[109,110] Instead of associating helices using antiparallel crossovers in traditional multistranded origami strategy,[29] Yin and co-workers employed paranemic crossovers (PX) in their ssOrigami strategy to prevent the long single-stranded DNA from being knotted.[111] Additionally, other single-stranded origami design languages implementing 90° kinks and branched kissing-loops were proposed to build wireframe structures.[112,113] Notably, all of these works demonstrated that long single-stranded DNA or RNA can be replicated both *in vitro* and *in vivo*, but the assembly involves differentiated annealing steps. PX-based origami necessitates a thermo-annealing program starting at 85 °C, which is unavailable during cell cultivation. Albeit, RNA origami from Geary et al. realized the isothermal cotranscriptional folding *in vitro* at 37 °C,[109] and wireframe RNA structures were further shown to successfully fold within living cells, as confirmed by AFM images of cell lysates.[112,113] We believe that this discrepancy likely arises from the lack of self-complementary sequences within each of the two half RNA fragments in PX-based designs, resulting in the inability to form correctly folded local hairpins or stems during tran-

https://doi.org/10.1021/jacsau.4c00986
JACS Au 2025, 5, 17−27

scription. As a result, complete denaturation is favored to melt all secondary structures, allowing for the pairing of two half fragments. Continuous efforts in structural designing to minimize spurious local kinetic traps during cotranscriptional *in situ* folding will be beneficial for creating more delicate Nanotags. Inspiration can also be drawn from the mechanisms of protein folding, as proteins are similarly folded by a single chain of polypeptides within living cells.[111]

To specifically label a POI, a variety of ligands can be attached to the Nanotags. Options include peptides,[114] antibodies,[58] self-labeling protein tags,[115] small molecular ligands,[116] and bio-orthogonal functional groups.[117] These modifications, however, are not applicable to *in situ* expressed and folded RNA Nanotags. Alternatively, short, single-stranded nucleic acid aptamers can serve as affinity labels for Nanotags.[118] A caveat for using aptamers is that the conditional aptamer discovery pipeline requires intensive efforts, with no guarantee that high-affinity aptamers can always be obtained for any given POI.[119] Exploiting existing aptamers that target recombinant protein tags[120,121] is a simple yet efficient solution that circumvents the *de novo* selection of unique aptamers. For example, the "SPOTs" target sfGFP-fused gB by integrating a high-affinity GFP-binding aptamer.[19] However, other attempts, such as using aptamer against hexahistidine tags, were less successful,[19] highlighting the need for more robust aptamers against common protein fusion tags.

Another concern is that off-target Nanotags may be misidentified as correctly targeted ones during data processing, compromising their labeling accuracy and increasing the false-positive rate. Besides genetically regulating the expression level of the Nanotag-carrying plasmid, constructing a target-responsive allosteric nanostructure could be one feasible solution to screen the positively tagged Nanotags in the cellular matrix. For example, ligand-responsive aptamer switch architectures can elicit conformational change and strand displacement of nucleic acid molecules.[122] These aptamers can trigger the conformational change of origami nanodevices,[123,124] allowing the accurate recognition and separation of target particles in cryo-ET data sets.

INTRACELLULAR MIGRATION AND TARGETING

Targeted delivery of DNA nanostructures to specific organelles is primarily achieved by attaching organelle-targeting peptides (OTPs) such as nuclear targeting sequence (NTS) peptides, N-(βA)VVVKKKRKVVC, and mitochondrial targeting sequence (MTS) peptides, N-(βA)LLYRSSCLTRTAPKFRISQRLSLM,[101] to these constructs. The distribution of DNA nanocages within subcellular organelles was observed through the colocalization of dye-labeled DNA nanostructures and specifically stained cellular organelles.[101] Alternatively, caveolae-mediated endocytosis (CvME) allows endocytic carriers to either fuse with early endosomes or transfer directly to the ER via caveosomes,[125] potentially enabling ER delivery without the need for related OTPs.[126,127]

Given that the cytoplasm is a highly complex, multiphase system with spatial heterogeneity,[128] enhancing the diffusion of Nanotags becomes particularly critical for achieving rapid cytosolic trafficking. Typically, nanoparticle diffusion is influenced by the intrinsic properties of both the surrounding matrix[128] (such as pore size, solid content, viscosity, etc.) and the nanoparticles themselves (such as size,[129] aspect ratio,[130,131] etc.), as well as their mutual interactions.[128] Both theoretical models[132,133] and experimental evidence[129] suggest that smaller nanoparticles encounter less resistance from the matrix and therefore diffuse more rapidly. Additionally, passivating the nanoparticle surface to reduce nonspecific interactions with cellular components is essential for ensuring the particles reach their intended targets efficiently.[134] Nevertheless, the migration behavior of DNA nanostructures has not yet been systematically studied. While trends observed in other types of nanoparticles are helpful, the unique properties of DNA Nanotags, such as strong negative charge and delicate programmability of shapes (e.g., varying twist angles and handedness[33]), introduce factors that could affect their intracellular migration. Studying DNA Nanotag migration directly within living cells could better mirror real-world conditions. Alternatively, simplified analog networks, such as DNA supramolecular hydrogels[135] or extracellular matrices,[136] can be employed for single-factor analyses. Real-time observation techniques, such as single-particle tracking (SPT),[137,138] offer valuable insights into dynamics information by extracting key parameters, including mean square displacement (MSD) and diffusion coefficients,[139] enabling the characterization of particle diffusion rates. Additional experimental results with simulations could help identify trends that aid the rational design of DNA Nanotags and optimize their migration for *in situ* cryo-ET applications.

SUMMARY AND OUTLOOK

DNA nanostructures offer unique shapes than "blob-like" protein particles and demonstrate compatibility with standard cryo-EM protocols, including the ability to conjugate with biomolecules and withstand various sample preparation conditions. Building on these advantages, this article explores an emerging application of DNA nanostructures: DNA Nanotags—molecular markers specifically designed to label proteins.

By parallelly labeling protein complexes with distinct Nanotags, these markers enable the identification of multiple targets within a single EM grid, facilitating high-throughput multiplexed EM imaging. EM-visible Nanotags are also anticipated to accurately localize target particles from low SNR cryo-ET data sets of crowded cellular landscapes. However, the successful integration of DNA Nanotags into *in situ* applications requires overcoming challenges related to cellular uptake and intracellular trafficking. Platforms for the direct cytosolic delivery of mRNA and plasmids present promising strategies for delivering DNA Nanotags. Additionally, the potential for *in situ* expression of ssOrigami offers an innovative alternative. For the second challenge, although current reports on the intracellular migration of DNA nanostructures are limited, insights can be gleaned from simulations and the *in vivo* diffusion behavior of other nanoparticles. Another concern is the stimulation of immune pathways by DNA, including TLR9,[140] cGAS/STING[141] and AIM2.[142] However, the extent of the intracellular immune response elicited by DNA nanostructures has not been explored. Consequently, the potential impact of Nanotags on the native cellular environment should be carefully evaluated to determine whether they affect the intended targets of interest.

Despite these challenges, future optimizations toward assembly and modification processes of DNA Nanotags will be necessary to ensure robust stability and simpler usage, paving the way for the development of ready-to-use protein-labeling kits for widespread adoption in structural biology laboratories. In addition to their applications in structural

https://doi.org/10.1021/jacsau.4c00986
JACS Au 2025, 5, 17−27

biology, DNA Nanotags can serve as valuable tools for investigating various physiological mechanisms. For instance, tomograms reconstructed with "signposts" (Figure 1E) highlight the potential application of DNA Nanotags in mapping the distribution of exposed protein epitopes[143] on the surface of the protein corona, cell, and other structures.

AUTHOR INFORMATION

Corresponding Author

Yuhe R. Yang − *CAS Key Laboratory of Nanosystem and Hierarchical Fabrication, CAS Center for Excellence in Nanoscience, National Center for Nanoscience and Technology of China, CAS, Beijing 100190, China; University of Chinese Academy of Sciences, Beijing 100049, China;* orcid.org/0000-0003-2321-4653; Email: yangyh@nanoctr.cn

Authors

Yuanfang Chen − *CAS Key Laboratory of Nanosystem and Hierarchical Fabrication, CAS Center for Excellence in Nanoscience, National Center for Nanoscience and Technology of China, CAS, Beijing 100190, China; University of Chinese Academy of Sciences, Beijing 100049, China;* orcid.org/0000-0002-4404-5302

Yiqian Huang − *CAS Key Laboratory of Nanosystem and Hierarchical Fabrication, CAS Center for Excellence in Nanoscience, National Center for Nanoscience and Technology of China, CAS, Beijing 100190, China; University of Chinese Academy of Sciences, Beijing 100049, China*

Complete contact information is available at: https://pubs.acs.org/10.1021/jacsau.4c00986

Author Contributions

#Y.C. and Y.H. contributed equally.

Notes

The authors declare no competing financial interest.

ACKNOWLEDGMENTS

This work was supported by National Key R&D Program of China (2022YFA1206400); the National Natural Science Foundation of China (22277017).

REFERENCES

(1) Nakane, T.; Kotecha, A.; Sente, A.; McMullan, G.; Masiulis, S.; Brown, P.; Grigoras, I. T.; Malinauskaite, L.; Malinauskas, T.; Miehling, J.; et al. Single-particle cryo-EM at atomic resolution. *Nature* **2020**, *587* (7832), 152−156.

(2) Yonekura, K.; Maki-Yonekura, S.; Naitow, H.; Hamaguchi, T.; Takaba, K. Machine learning-based real-time object locator/evaluator for cryo-EM data collection. *Commun. Biol.* **2021**, *4* (1), 1044.

(3) Zhang, X.; Johnson, R. M.; Drulyte, I.; Yu, L.; Kotecha, A.; Danev, R.; Wootten, D.; Sexton, P. M.; Belousoff, M. J. Evolving cryo-EM structural approaches for GPCR drug discovery. *Structure* **2021**, *29* (9), 963−974.

(4) Renaud, J. P.; Chari, A.; Ciferri, C.; Liu, W. T.; Remigy, H. W.; Stark, H.; Wiesmann, C. Cryo-EM in drug discovery: achievements, limitations and prospects. *Nat. Rev. Drug Discov* **2018**, *17* (7), 471−492.

(5) Wacker, D.; Stevens, R. C.; Roth, B. L. How Ligands Illuminate GPCR Molecular Pharmacology. *Cell* **2017**, *170* (3), 414−427.

(6) Mulligan, S. K.; Speir, J. A.; Razinkov, I.; Cheng, A.; Crum, J.; Jain, T.; Duggan, E.; Liu, E.; Nolan, J. P.; Carragher, B.; et al. Multiplexed TEM Specimen Preparation and Analysis of Plasmonic Nanoparticles. *Microsc Microanal* **2015**, *21* (4), 1017−1025.

(7) Jain, T.; Sheehan, P.; Crum, J.; Carragher, B.; Potter, C. S. Spotiton: a prototype for an integrated inkjet dispense and vitrification system for cryo-TEM. *J. Struct Biol.* **2012**, *179* (1), 68−75.

(8) Razinkov, I.; Dandey, V.; Wei, H.; Zhang, Z.; Melnekoff, D.; Rice, W. J.; Wigge, C.; Potter, C. S.; Carragher, B. A new method for vitrifying samples for cryoEM. *J. Struct Biol.* **2016**, *195* (2), 190−198.

(9) Dandey, V. P.; Wei, H.; Zhang, Z.; Tan, Y. Z.; Acharya, P.; Eng, E. T.; Rice, W. J.; Kahn, P. A.; Potter, C. S.; Carragher, B. Spotiton: New features and applications. *J. Struct Biol.* **2018**, *202* (2), 161−169.

(10) Dandey, V. P.; Budell, W. C.; Wei, H.; Bobe, D.; Maruthi, K.; Kopylov, M.; Eng, E. T.; Kahn, P. A.; Hinshaw, J. E.; Kundu, N.; et al. Time-resolved cryo-EM using Spotiton. *Nat. Methods* **2020**, *17* (9), 897−900.

(11) Carlson, B. M. Cells. In *The Human Body*; Carlson, B. M., Ed.; Academic Press, 2019; pp 1−25.

(12) Kikkawa, M.; Yanagisawa, H. Identifying proteins in the cell by tagging techniques for cryo-electron microscopy. *Microscopy (Oxf)* **2022**, *71* (Supplement_1), i60−i65.

(13) Bos, E.; Hussaarts, L.; van Weering, J. R.; Ellisman, M. H.; de Wit, H.; Koster, A. J. Vitrification of Tokuyasu-style immuno-labelled sections for correlative cryo light microscopy and cryo electron tomography. *J. Struct Biol.* **2014**, *186* (2), 273−282.

(14) Yi, H.; Strauss, J. D.; Ke, Z.; Alonas, E.; Dillard, R. S.; Hampton, C. M.; Lamb, K. M.; Hammonds, J. E.; Santangelo, P. J.; Spearman, P. W.; et al. Native immunogold labeling of cell surface proteins and viral glycoproteins for cryo-electron microscopy and cryo-electron tomography applications. *J. Histochem Cytochem* **2015**, *63* (10), 780−792.

(15) Jiang, Z.; Jin, X.; Li, Y.; Liu, S.; Liu, X. M.; Wang, Y. Y.; Zhao, P.; Cai, X.; Liu, Y.; Tang, Y.; et al. Genetically encoded tags for direct synthesis of EM-visible gold nanoparticles in cells. *Nat. Methods* **2020**, *17* (9), 937−946.

(16) Wang, Q.; Mercogliano, C. P.; Lowe, J. A ferritin-based label for cellular electron cryotomography. *Structure* **2011**, *19* (2), 147−154.

(17) Clarke, N. I.; Royle, S. J. FerriTag is a new genetically-encoded inducible tag for correlative light-electron microscopy. *Nat. Commun.* **2018**, *9* (1), 2604.

(18) Wang, C.; Iacovache, I.; Zuber, B.Genetically Encoded FerriTag as a Specific Label for Cryo-Electron Tomography. *bioRxiv*, 2024. DOI: 10.1101/2024.09.10.612178.

(19) Silvester, E.; Vollmer, B.; Prazak, V.; Vasishtan, D.; Machala, E. A.; Whittle, C.; Black, S.; Bath, J.; Turberfield, A. J.; Grunewald, K.; et al. DNA origami signposts for identifying proteins on cell membranes by electron cryotomography. *Cell* **2021**, *184* (4), 1110−1121.

(20) Sun, W. W.; Michalak, D. J.; Sochacki, K. A.; Kunamaneni, P.; Alfonzo-Méndez, M. A.; Arnold, A. M.; Strub, M.-P.; Hinshaw, J. E.; Taraska, J. W. Cryo-electron tomography pipeline for plasma membranes. *bioRxiv*, 2024. DOI: 10.1101/2024.06.27.600657.

(21) Fung, H. K. H.; Hayashi, Y.; Salo, V. T.; Babenko, A.; Zagoriy, I.; Brunner, A.; Ellenberg, J.; Muller, C. W.; Cuylen-Haering, S.; Mahamid, J. Genetically encoded multimeric tags for subcellular protein localization in cryo-EM. *Nat. Methods* **2023**, *20* (12), 1900−1908.

(22) Henderson, R. Avoiding the pitfalls of single particle cryo-electron microscopy: Einstein from noise. *Proc. Natl. Acad. Sci. U. S. A.* **2013**, *110* (45), 18037−18041.

(23) Seeman, N. C. Nucleic acid junctions and lattices. *J. Theor. Biol.* **1982**, *99* (2), 237−247.

(24) Kallenbach, N. R.; Ma, R. I.; Seeman, N. C. An Immobile Nucleic-Acid Junction Constructed from Oligonucleotides. *Nature* **1983**, *305* (5937), 829−831.

(25) Winfree, E.; Liu, F.; Wenzler, L. A.; Seeman, N. C. Design and self-assembly of two-dimensional DNA crystals. *Nature* **1998**, *394* (6693), 539−544.

(26) Yan, H.; Park, S. H.; Finkelstein, G.; Reif, J. H.; LaBean, T. H. DNA-templated self-assembly of protein arrays and highly conductive nanowires. *Science* **2003**, *301* (5641), 1882−1884.
(27) Shih, W. M.; Quispe, J. D.; Joyce, G. F. A 1.7-kilobase single-stranded DNA that folds into a nanoscale octahedron. *Nature* **2004**, *427* (6975), 618−621.
(28) He, Y.; Ye, T.; Su, M.; Zhang, C.; Ribbe, A. E.; Jiang, W.; Mao, C. Hierarchical self-assembly of DNA into symmetric supramolecular polyhedra. *Nature* **2008**, *452* (7184), 198−201.
(29) Rothemund, P. W. Folding DNA to create nanoscale shapes and patterns. *Nature* **2006**, *440* (7082), 297−302.
(30) Douglas, S. M.; Dietz, H.; Liedl, T.; Högberg, B.; Graf, F.; Shih, W. M. Self-assembly of DNA into nanoscale three-dimensional shapes. *Nature* **2009**, *459* (7245), 414−418.
(31) Ke, Y.; Douglas, S. M.; Liu, M.; Sharma, J.; Cheng, A.; Leung, A.; Liu, Y.; Shih, W. M.; Yan, H. Multilayer DNA origami packed on a square lattice. *J. Am. Chem. Soc.* **2009**, *131* (43), 15903−15908.
(32) Ke, Y.; Voigt, N. V.; Gothelf, K. V.; Shih, W. M. Multilayer DNA origami packed on hexagonal and hybrid lattices. *J. Am. Chem. Soc.* **2012**, *134* (3), 1770−1774.
(33) Dietz, H.; Douglas, S. M.; Shih, W. M. Folding DNA into twisted and curved nanoscale shapes. *Science* **2009**, *325* (5941), 725−730.
(34) Han, D.; Pal, S.; Nangreave, J.; Deng, Z.; Liu, Y.; Yan, H. DNA origami with complex curvatures in three-dimensional space. *Science* **2011**, *332* (6027), 342−346.
(35) Wei, B.; Dai, M.; Yin, P. Complex shapes self-assembled from single-stranded DNA tiles. *Nature* **2012**, *485* (7400), 623−626.
(36) Ke, Y.; Ong, L. L.; Shih, W. M.; Yin, P. Three-dimensional structures self-assembled from DNA bricks. *Science* **2012**, *338* (6111), 1177−1183.
(37) Jun, H.; Shepherd, T. R.; Zhang, K.; Bricker, W. P.; Li, S.; Chiu, W.; Bathe, M. Automated Sequence Design of 3D Polyhedral Wireframe DNA Origami with Honeycomb Edges. *ACS Nano* **2019**, *13* (2), 2083−2093.
(38) Fu, D.; Pradeep Narayanan, R.; Prasad, A.; Zhang, F.; Williams, D.; Schreck, J. S.; Yan, H.; Reif, J. Automated design of 3D DNA origami with non-rasterized 2D curvature. *Sci. Adv.* **2022**, *8* (51), No. eade4455.
(39) Lolaico, M.; Blokhuizen, S.; Shen, B.; Wang, Y.; Hogberg, B. Computer-Aided Design of A-Trail Routed Wireframe DNA Nanostructures with Square Lattice Edges. *ACS Nano* **2023**, *17* (7), 6565−6574.
(40) Dong, Y.; Chen, S.; Zhang, S.; Sodroski, J.; Yang, Z.; Liu, D.; Mao, Y. Folding DNA into a Lipid-Conjugated Nanobarrel for Controlled Reconstitution of Membrane Proteins. *Angew. Chem., Int. Ed. Engl.* **2018**, *57* (8), 2072−2076.
(41) Fu, J.; Yang, Y. R.; Dhakal, S.; Zhao, Z.; Liu, M.; Zhang, T.; Walter, N. G.; Yan, H. Assembly of multienzyme complexes on DNA nanostructures. *Nat. Protoc* **2016**, *11* (11), 2243−2273.
(42) Fu, J.; Li, T. Spatial Organization of Enzyme Cascade on a DNA Origami Nanostructure. In *3D DNA Nanostructure: Methods and Protocols*; Ke, Y.; Wang, P., Eds.; Springer New York, 2017; pp 153−164.
(43) Benson, E.; Mohammed, A.; Gardell, J.; Masich, S.; Czeizler, E.; Orponen, P.; Hogberg, B. DNA rendering of polyhedral meshes at the nanoscale. *Nature* **2015**, *523* (7561), 441−444.
(44) Veneziano, R.; Ratanalert, S.; Zhang, K.; Zhang, F.; Yan, H.; Chiu, W.; Bathe, M. Designer nanoscale DNA assemblies programmed from the top down. *Science* **2016**, *352* (6293), 1534.
(45) Kielar, C.; Xin, Y.; Shen, B.; Kostiainen, M. A.; Grundmeier, G.; Linko, V.; Keller, A. On the Stability of DNA Origami Nanostructures in Low-Magnesium Buffers. *Angew. Chem., Int. Ed. Engl.* **2018**, *57* (30), 9470−9474.
(46) Perrault, S. D.; Shih, W. M. Virus-inspired membrane encapsulation of DNA nanostructures to achieve in vivo stability. *ACS Nano* **2014**, *8* (5), 5132−5140.
(47) Mikkilä, J.; Eskelinen, A.-P.; Niemelä, E. H.; Linko, V.; Frilander, M. J.; Törmä, P.; Kostiainen, M. A. Virus-Encapsulated DNA Origami Nanostructures for Cellular Delivery. *Nano Lett.* **2014**, *14* (4), 2196−2200.
(48) Ponnuswamy, N.; Bastings, M. M. C.; Nathwani, B.; Ryu, J. H.; Chou, L. Y. T.; Vinther, M.; Li, W. A.; Anastassacos, F. M.; Mooney, D. J.; Shih, W. M. Oligolysine-based coating protects DNA nanostructures from low-salt denaturation and nuclease degradation. *Nat. Commun.* **2017**, *8* (1), 15654.
(49) Wang, Y.; Baars, I.; Berzina, I.; Rocamonde-Lago, I.; Shen, B.; Yang, Y.; Lolaico, M.; Waldvogel, J.; Smyrlaki, I.; Zhu, K.; et al. A DNA robotic switch with regulated autonomous display of cytotoxic ligand nanopatterns. *Nat. Nanotechnol* **2024**, *19* (9), 1366−1374.
(50) Ramakrishnan, S.; Ijas, H.; Linko, V.; Keller, A. Structural stability of DNA origami nanostructures under application-specific conditions. *Comput. Struct Biotechnol J.* **2018**, *16*, 342−349.
(51) Zhang, K.; Julius, D.; Cheng, Y. A step-by-step protocol for capturing conformational snapshots of ligand gated ion channels by single-particle cryo-EM. *STAR Protoc* **2022**, *3* (4), 101732.
(52) Selmi, D. N.; Adamson, R. J.; Attrill, H.; Goddard, A. D.; Gilbert, R. J.; Watts, A.; Turberfield, A. J. DNA-templated protein arrays for single-molecule imaging. *Nano Lett.* **2011**, *11* (2), 657−660.
(53) Martin, T. G.; Bharat, T. A.; Joerger, A. C.; Bai, X. C.; Praetorius, F.; Fersht, A. R.; Dietz, H.; Scheres, S. H. Design of a molecular support for cryo-EM structure determination. *Proc. Natl. Acad. Sci. U. S. A.* **2016**, *113* (47), No. E7456-E7463.
(54) Aksel, T.; Yu, Z.; Cheng, Y.; Douglas, S. M. Molecular goniometers for single-particle cryo-electron microscopy of DNA-binding proteins. *Nat. Biotechnol.* **2021**, *39* (3), 378−386.
(55) Aissaoui, N.; Lai-Kee-Him, J.; Mills, A.; Declerck, N.; Morichaud, Z.; Brodolin, K.; Baconnais, S.; Le Cam, E.; Charbonnier, J. B.; Sounier, R.; et al. Modular Imaging Scaffold for Single-Particle Electron Microscopy. *ACS Nano* **2021**, *15* (3), 4186−4196.
(56) Kuhlbrandt, W. Biochemistry. The resolution revolution. *Science* **2014**, *343* (6178), 1443−1444.
(57) Cremers, G. A. O.; Rosier, B.; Meijs, A.; Tito, N. B.; van Duijnhoven, S. M. J.; van Eenennaam, H.; Albertazzi, L.; de Greef, T. F. A. Determinants of Ligand-Functionalized DNA Nanostructure-Cell Interactions. *J. Am. Chem. Soc.* **2021**, *143* (27), 10131−10142.
(58) Wagenbauer, K. F.; Pham, N.; Gottschlich, A.; Kick, B.; Kozina, V.; Frank, C.; Trninic, D.; Stommer, P.; Grunmeier, R.; Carlini, E.; et al. Programmable multispecific DNA-origami-based T-cell engagers. *Nat. Nanotechnol* **2023**, *18* (11), 1319−1326.
(59) Wamhoff, E. C.; Ronsard, L.; Feldman, J.; Knappe, G. A.; Hauser, B. M.; Romanov, A.; Case, J. B.; Sanapala, S.; Lam, E. C.; Denis, K. J. S.; et al. Enhancing antibody responses by multivalent antigen display on thymus-independent DNA origami scaffolds. *Nat. Commun.* **2024**, *15* (1), 795.
(60) Ge, Z.; Su, Z.; Simmons, C. R.; Li, J.; Jiang, S.; Li, W.; Yang, Y.; Liu, Y.; Chiu, W.; Fan, C.; et al. Redox Engineering of Cytochrome c using DNA Nanostructure-Based Charged Encapsulation and Spatial Control. *ACS Appl. Mater. Interfaces* **2019**, *11* (15), 13874−13880.
(61) Huang, J.; Jaekel, A.; van den Boom, J.; Podlesainski, D.; Elnaggar, M.; Heuer-Jungemann, A.; Kaiser, M.; Meyer, H.; Sacca, B. A modular DNA origami nanocompartment for engineering a cell-free, protein unfolding and degradation pathway. *Nat. Nanotechnol* **2024**, *19* (10), 1521−1531.
(62) Abels, J. A.; Moreno-Herrero, F.; van der Heijden, T.; Dekker, C.; Dekker, N. H. Single-molecule measurements of the persistence length of double-stranded RNA. *Biophys. J.* **2005**, *88* (4), 2737−2744.
(63) Praetorius, F.; Dietz, H. Self-assembly of genetically encoded DNA-protein hybrid nanoscale shapes. *Science* **2017**, *355* (6331), No. eaam5488.
(64) Zhou, X.; Li, Y.; Zhang, C.; Zheng, W.; Zhang, G.; Zhang, Y. Progressive assembly of multi-domain protein structures from cryo-EM density maps. *Nat. Comput. Sci.* **2022**, *2* (4), 265−275.
(65) Reddy Chichili, V. P.; Kumar, V.; Sivaraman, J. Linkers in the structural biology of protein-protein interactions. *Protein Sci.* **2013**, *22* (2), 153−167.

https://doi.org/10.1021/jacsau.4c00986
JACS Au 2025, 5, 17−27

(66) Chai, P. X.; Rao, Q. H.; Zhang, K. Multi-curve fitting and tubulin-lattice signal removal for structure determination of large microtubule-based motors. *J. Struct. Biol.* **2022**, *214* (4), 107897.
(67) Chai, P.; Rao, Q.; Wang, Y.; Zhang, K. High-Resolution Structural Analysis of Dyneins by Cryo-electron Microscopy. In *Dynein*; Markus, S. M., Ed.; Methods in Molecular Biology; Springer US, 2023; pp 257−279.
(68) Zheng, W.; Chai, P.; Zhu, J.; Zhang, K. High-resolution in situ structures of mammalian respiratory supercomplexes. *Nature* **2024**, *631* (8019), 232−239.
(69) Dou, T.; Lian, T.; Shu, S.; He, Y.; Jiang, J. The substrate and inhibitor binding mechanism of polyspecific transporter OAT1 revealed by high-resolution cryo-EM. *Nat. Struct Mol. Biol.* **2023**, *30* (11), 1794−1805.
(70) Bohm, J.; Frangakis, A. S.; Hegerl, R.; Nickell, S.; Typke, D.; Baumeister, W. Toward detecting and identifying macromolecules in a cellular context: template matching applied to electron tomograms. *Proc. Natl. Acad. Sci. U. S. A.* **2000**, *97* (26), 14245−14250.
(71) Jin, W.; Zhou, Y.; Bartesaghi, A. Accurate size-based protein localization from cryo-ET tomograms. *J. Struct Biol. X* **2024**, *10*, 100104.
(72) Rastogi, A. Particle picking in tomograms. *Nat. Comput. Sci.* **2023**, *3* (6), 476.
(73) McIntosh, R.; Nicastro, D.; Mastronarde, D. New views of cells in 3D: an introduction to electron tomography. *Trends Cell Biol.* **2005**, *15* (1), 43−51.
(74) Liu, G.; Niu, T.; Qiu, M.; Zhu, Y.; Sun, F.; Yang, G. DeepETPicker: Fast and accurate 3D particle picking for cryo-electron tomography using weakly supervised deep learning. *Nat. Commun.* **2024**, *15* (1), 2090.
(75) Bai, X. C.; Martin, T. G.; Scheres, S. H. W.; Dietz, H. Cryo-EM structure of a 3D DNA-origami object. *P Natl. Acad. Sci. USA* **2012**, *109* (49), 20012−20017.
(76) Manzanares, D.; Cena, V. Endocytosis: The Nanoparticle and Submicron Nanocompounds Gateway into the Cell. *Pharmaceutics* **2020**, *12* (4), 371.
(77) Wang, Y.; Benson, E.; Fördös, F.; Lolaico, M.; Baars, I.; Fang, T.; Teixeira, A. I.; Högberg, B. DNA Origami Penetration in Cell Spheroid Tissue Models is Enhanced by Wireframe Design. *Adv. Mater.* **2021**, *33* (29), 2008457.
(78) Wang, P.; Rahman, M. A.; Zhao, Z.; Weiss, K.; Zhang, C.; Chen, Z.; Hurwitz, S. J.; Chen, Z. G.; Shin, D. M.; Ke, Y. Visualization of the Cellular Uptake and Trafficking of DNA Origami Nanostructures in Cancer Cells. *J. Am. Chem. Soc.* **2018**, *140* (7), 2478−2484.
(79) Bastings, M. M. C.; Anastassacos, F. M.; Ponnuswamy, N.; Leifer, F. G.; Cuneo, G.; Lin, C.; Ingber, D. E.; Ryu, J. H.; Shih, W. M. Modulation of the Cellular Uptake of DNA Origami through Control over Mass and Shape. *Nano Lett.* **2018**, *18* (6), 3557−3564.
(80) Maezawa, T.; Ohtsuki, S.; Hidaka, K.; Sugiyama, H.; Endo, M.; Takahashi, Y.; Takakura, Y.; Nishikawa, M. DNA density-dependent uptake of DNA origami-based two-or three-dimensional nanostructures by immune cells. *Nanoscale* **2020**, *12* (27), 14818−14824.
(81) Ding, H.; Li, J.; Chen, N.; Hu, X.; Yang, X.; Guo, L.; Li, Q.; Zuo, X.; Wang, L.; Ma, Y.; et al. DNA Nanostructure-Programmed Like-Charge Attraction at the Cell-Membrane Interface. *ACS Central Science* **2018**, *4* (10), 1344−1351.
(82) Sun, W.; Ji, W.; Hall, J. M.; Hu, Q.; Wang, C.; Beisel, C. L.; Gu, Z. Self-Assembled DNA Nanoclews for the Efficient Delivery of CRISPR-Cas9 for Genome Editing. *Angew. Chem.* **2015**, *127* (41), 12197−12201.
(83) Xu, X.; Fang, S.; Zhuang, Y.; Wu, S.; Pan, Q.; Li, L.; Wang, X.; Sun, X.; Liu, B.; Wu, Y. Cationic Albumin Encapsulated DNA Origami for Enhanced Cellular Transfection and Stability. *Materials* **2019**, *12* (6), 949.
(84) Singh, R.; Yadav, P.; Naveena A, H.; Bhatia, D. Cationic lipid modification of DNA tetrahedral nanocages enhances their cellular uptake. *Nanoscale* **2023**, *15* (3), 1099−1108.
(85) Wu, X.; Yang, C.; Wang, H.; Lu, X.; Shang, Y.; Liu, Q.; Fan, J.; Liu, J.; Ding, B. Genetically Encoded DNA Origami for Gene Therapy In Vivo. *J. Am. Chem. Soc.* **2023**, *145* (16), 9343−9353.
(86) Li, Y. J.; Yuan, W.; Tian, X. C.; Zhu, C. Y.; Li, X.; Chen, R. F.; Hao, Z. Y.; Dong, Y. C.; Liu, D. S. A facile method to prepare non-cationic mRNA lipid-nanoparticles based on frame guided assembly strategy. *Nano Today* **2023**, *52*, 101991.
(87) Khmelinskaia, A.; Mücksch, J.; Petrov, E. P.; Franquelim, H. G.; Schwille, P. Control of Membrane Binding and Diffusion of Cholesteryl-Modified DNA Origami Nanostructures by DNA Spacers. *Langmuir* **2018**, *34* (49), 14921−14931.
(88) Liu, Y.; Wijesekara, P.; Kumar, S.; Wang, W.; Ren, X.; Taylor, R. E. The effects of overhang placement and multivalency on cell labeling by DNA origami. *Nanoscale* **2021**, *13* (14), 6819−6828.
(89) Wang, W.; Chopra, B.; Walawalkar, V.; Liang, Z.; Adams, R.; Deserno, M.; Ren, X.; Taylor, R. E. Cell-Surface Binding of DNA Nanostructures for Enhanced Intracellular and Intranuclear Delivery. *ACS Appl. Mater. Interfaces* **2024**, *16* (13), 15783−15797.
(90) Schaffert, D. H.; Okholm, A. H.; Sørensen, R. S.; Nielsen, J. S.; Tørring, T.; Rosen, C. B.; Kodal, A. L. B.; Mortensen, M. R.; Gothelf, K. V.; Kjems, J. Intracellular Delivery of a Planar DNA Origami Structure by the Transferrin-Receptor Internalization Pathway. *Small* **2016**, *12* (19), 2634−2640.
(91) Lee, H.; Lytton-Jean, A. K. R.; Chen, Y.; Love, K. T.; Park, A. I.; Karagiannis, E. D.; Sehgal, A.; Querbes, W.; Zurenko, C. S.; Jayaraman, M.; et al. Molecularly self-assembled nucleic acid nanoparticles for targeted in vivo siRNA delivery. *Nat. Nanotechnol.* **2012**, *7* (6), 389−393.
(92) Ko, S.; Liu, H.; Chen, Y.; Mao, C. DNA Nanotubes as Combinatorial Vehicles for Cellular Delivery. *Biomacromolecules* **2008**, *9* (11), 3039−3043.
(93) Charoenphol, P.; Bermudez, H. Aptamer-Targeted DNA Nanostructures for Therapeutic Delivery. *Mol. Pharmaceutics* **2014**, *11* (5), 1721−1725.
(94) Udomprasert, A.; Wootthichairangsan, C.; Duangrat, R.; Chaithongyot, S.; Zhang, Y.; Nixon, R.; Liu, W.; Wang, R.; Ponglikitmongkol, M.; Kangsamaksin, T. Enhanced Functional Properties of Three DNA Origami Nanostructures as Doxorubicin Carriers to Breast Cancer Cells. *ACS Applied Bio Materials* **2022**, *5* (5), 2262−2272.
(95) Xia, Z.; Wang, P.; Liu, X.; Liu, T.; Yan, Y.; Yan, J.; Zhong, J.; Sun, G.; He, D. Tumor-Penetrating Peptide-Modified DNA Tetrahedron for Targeting Drug Delivery. *Biochemistry* **2016**, *55* (9), 1326−1331.
(96) Voltà-Durán, E.; Parladé, E.; Serna, N.; Villaverde, A.; Vazquez, E.; Unzueta, U. Endosomal escape for cell-targeted proteins. Going out after going in. *Biotechnology Advances* **2023**, *63*, 108103.
(97) Tang, W.; Tong, T.; Wang, H.; Lu, X.; Yang, C.; Wu, Y.; Wang, Y.; Liu, J.; Ding, B. A DNA Origami-Based Gene Editing System for Efficient Gene Therapy in Vivo. *Angew. Chem., Int. Ed. Engl.* **2023**, *62* (51), No. e202315093.
(98) Smolková, B.; MacCulloch, T.; Rockwood, T. F.; Liu, M.; Henry, S. J. W.; Frtús, A.; Uzhytchak, M.; Lunova, M.; Hof, M.; Jurkiewicz, P.; et al. Protein Corona Inhibits Endosomal Escape of Functionalized DNA Nanostructures in Living Cells. *ACS Appl. Mater. Interfaces* **2021**, *13* (39), 46375−46390.
(99) He, J.; Ji, X.; Xu, Z.; He, W.; Zhao, Y.; Sun, L.; Ma, L. Coating tetrahedral DNA framework with endosomolytic peptides for improved stability and cytosolic delivery. *Advanced Sensor and Energy Materials* **2024**, *3* (2), 100098.
(100) Chopra, A.; Krishnan, S.; Simmel, F. C. Electrotransfection of Polyamine Folded DNA Origami Structures. *Nano Lett.* **2016**, *16* (10), 6683−6690.
(101) Chan, M. S.; Lo, P. K. Nanoneedle-Assisted Delivery of Site-Selective Peptide-Functionalized DNA Nanocages for Targeting Mitochondria and Nuclei. *Small* **2014**, *10* (7), 1255−1260.
(102) Nikolov, P. M.; Koßmann, K. J.; Schilling, A.; Angelin, A.; Brglez, J.; Klein, A.; Tampé, R.; Rabe, K. S.; Niemeyer, C. M.

Cytosolic delivery of large supramolecular protein complexes arranged on DNA nanopegboards. *bioRxiv*, 2017. DOI: 10.1101/236729.
(103) Yu, L.; Xu, Y.; Al-Amin, M.; Jiang, S.; Sample, M.; Prasad, A.; Stephanopoulos, N.; Šulc, P.; Yan, H. CytoDirect: A Nucleic Acid Nanodevice for Specific and Efficient Delivery of Functional Payloads to the Cytoplasm. *J. Am. Chem. Soc.* **2023**, *145* (50), 27336−27347.
(104) Brown, D. W.; Wee, P.; Bhandari, P.; Bukhari, A.; Grin, L.; Vega, H.; Hejazi, M.; Sosnowski, D.; Ablack, J.; Clancy, E. K.; et al. Safe and effective in vivo delivery of DNA and RNA using proteolipid vehicles. *Cell* **2024**, *187* (19), 5357−5375.
(105) Hu, Q.; Li, H.; Wang, L.; Gu, H.; Fan, C. DNA Nanotechnology-Enabled Drug Delivery Systems. *Chem. Rev.* **2019**, *119* (10), 6459−6506.
(106) Yang, W.; Liu, X.; Li, H.; Zhou, J.; Chen, S.; Wang, P.; Li, J.; Yang, H. Disulfide-Containing Molecular Sticker Assists Cellular Delivery of DNA Nanoassemblies by Bypassing Endocytosis. *CCS Chemistry* **2021**, *3* (3), 1178−1186.
(107) Youssef, S.; Tsang, E.; Samanta, A.; Kumar, V.; Gothelf, K. V. Reversible Protection and Targeted Delivery of DNA Origami with a Disulfide-Containing Cationic Polymer. *Small* **2024**, *20* (10), No. e2301058.
(108) Ciechonska, M.; Duncan, R. Reovirus FAST proteins: virus-encoded cellular fusogens. *Trends Microbiol* **2014**, *22* (12), 715−724.
(109) Geary, C.; Rothemund, P. W.; Andersen, E. S. A single-stranded architecture for cotranscriptional folding of RNA nanostructures. *Science* **2014**, *345* (6198), 799−804.
(110) Geary, C.; Grossi, G.; McRae, E. K. S.; Rothemund, P. W. K.; Andersen, E. S. RNA origami design tools enable cotranscriptional folding of kilobase-sized nanoscaffolds. *Nat. Chem.* **2021**, *13* (6), 549−558.
(111) Han, D.; Qi, X.; Myhrvold, C.; Wang, B.; Dai, M.; Jiang, S.; Bates, M.; Liu, Y.; An, B.; Zhang, F.; et al. Single-stranded DNA and RNA origami. *Science* **2017**, *358* (6369), No. eaao2648.
(112) Li, M.; Zheng, M.; Wu, S.; Tian, C.; Liu, D.; Weizmann, Y.; Jiang, W.; Wang, G.; Mao, C. In vivo production of RNA nanostructures via programmed folding of single-stranded RNAs. *Nat. Commun.* **2018**, *9* (1), 2196.
(113) Zhang, T. Q.; Qian, X. M.; Cui, H. C.; Li, Q. T.; Du, X. Y.; Fu, X. Y.; Gu, H. Z.; Zeng, W. W.; Wei, B. Y. Programmable in vitro and in vivo folding of single-stranded nucleic-acid wireframe origami. *Chem.* **2024**, *10* (8), 2550−2563.
(114) Sun, Y. Y.; Yan, L.; Sun, J. J.; Xiao, M. S.; Lai, W.; Song, G. Q.; Li, L.; Fan, C. H.; Pei, H. Nanoscale organization of two-dimensional multimeric pMHC reagents with DNA origami for CD8 T cell detection. *Nat. Commun.* **2022**, *13* (1), 3916.
(115) Nieves, D. J.; Hilzenrat, G.; Tran, J.; Yang, Z. M.; MacRae, H. H.; Baker, M. A. B.; Gooding, J. J.; Gaus, K. tagPAINT: covalent labelling of genetically encoded protein tags for DNA-PAINT imaging. *Roy Soc. Open Sci.* **2019**, *6* (12), 191268.
(116) Ge, Z. L.; Guo, L. J.; Wu, G. Q.; Li, J.; Sun, Y. L.; Hou, Y. Q.; Shi, J. Y.; Song, S. P.; Wang, L. H.; Fan, C. H.; et al. DNA Origami-Enabled Engineering of Ligand-Drug Conjugates for Targeted Drug Delivery. *Small* **2020**, *16* (16), 1904857.
(117) Wang, W. T.; Hayes, P. R.; Ren, X.; Taylor, R. E. Synthetic Cell Armor Made of DNA Origami. *Nano Lett.* **2023**, *23* (15), 7076−7085.
(118) Sakai, Y.; Islam, M. S.; Adamiak, M.; Shiu, S. C.; Tanner, J. A.; Heddle, J. G. DNA Aptamers for the Functionalisation of DNA Origami Nanostructures. *Genes-Basel* **2018**, *9* (12), 571.
(119) Zhou, J.; Rossi, J. Aptamers as targeted therapeutics: current potential and challenges. *Nat. Rev. Drug Discov* **2017**, *16* (3), 181−202.
(120) Sabrowski, W.; Dreymann, N.; Möller, A.; Czepluch, D.; Albani, P. P.; Theodoridis, D.; Menger, M. M. The use of high-affinity polyhistidine binders as masking probes for the selection of an NDM-1 specific aptamer. *Sci. Rep* **2022**, *12* (1), 7936.
(121) Yang, L. T.; Abudureheman, T.; Zheng, W. W.; Zhou, H.; Chen, J.; Duan, C. W.; Chen, K. M. A novel His-tag-binding aptamer for recombinant protein detection and T cell-based immunotherapy. *Talanta* **2023**, *263*, 124722.
(122) Rangel, A. E.; Hariri, A. A.; Eisenstein, M.; Soh, H. T. Engineering Aptamer Switches for Multifunctional Stimulus-Responsive Nanosystems. *Adv. Mater.* **2020**, *32* (50), No. e2003704.
(123) Li, S.; Jiang, Q.; Liu, S.; Zhang, Y.; Tian, Y.; Song, C.; Wang, J.; Zou, Y.; Anderson, G. J.; Han, J. Y.; et al. A DNA nanorobot functions as a cancer therapeutic in response to a molecular trigger in vivo. *Nat. Biotechnol.* **2018**, *36* (3), 258−264.
(124) Walter, H. K.; Bauer, J.; Steinmeyer, J.; Kuzuya, A.; Niemeyer, C. M.; Wagenknecht, H. A. "DNA Origami Traffic Lights" with a Split Aptamer Sensor for a Bicolor Fluorescence Readout. *Nano Lett.* **2017**, *17* (4), 2467−2472.
(125) Parton, R. G.; Simons, K. The multiple faces of caveolae. *Nat. Rev. Mol. Cell Biol.* **2007**, *8* (3), 185−194.
(126) Shi, Q.; Wu, Y.; Xu, Y.; Bao, M.; Chen, X.; Huang, K.; Yang, Q.; Yang, Y. Virus Mimetic Framework DNA as a Non-LNP Gene Carrier for Modulated Cell Endocytosis and Apoptosis. *ACS Nano* **2023**, *17* (3), 2460−2471.
(127) Liu, C. X.; Wang, B.; Zhu, W. P.; Xu, Y. F.; Yang, Y. Y.; Qian, X. H. An Endoplasmic Reticulum (ER)-Targeting DNA Nanodevice for Autophagy-Dependent Degradation of Proteins in Membrane-Bound Organelles. *Angew. Chem., Int. Ed. Engl.* **2022**, *61* (38), No. e202205509.
(128) Janczura, J.; Balcerek, M.; Burnecki, K.; Sabri, A.; Weiss, M.; Krapf, D. Identifying heterogeneous diffusion states in the cytoplasm by a hidden Markov model. *New J. Phys.* **2021**, *23* (5), 053018.
(129) Egloff, S.; Runser, A.; Klymchenko, A.; Reisch, A. Size-Dependent Electroporation of Dye-Loaded Polymer Nanoparticles for Efficient and Safe Intracellular Delivery. *Small Methods* **2021**, *5* (2), No. e2000947.
(130) Lee, B. J.; Cheema, Y.; Bader, S.; Duncan, G. A. Shaping nanoparticle diffusion through biological barriers to drug delivery. *JCIS Open* **2021**, *4*, 100025.
(131) Bao, C.; Liu, B.; Li, B.; Chai, J.; Zhang, L.; Jiao, L.; Li, D.; Yu, Z.; Ren, F.; Shi, X.; et al. Enhanced transport of shape and rigidity-tuned α-lactalbumin nanotubes across intestinal mucus and cellular barriers. *Nano Lett.* **2020**, *20* (2), 1352−1361.
(132) Brochard Wyart, F.; de Gennes, P.-G. Viscosity at small scales in polymer melts. *Eur. Phys. J. E* **2000**, *1* (1), 93−97.
(133) Amsden, B. An obstruction-scaling model for diffusion in homogeneous hydrogels. *Macromolecules* **1999**, *32* (3), 874−879.
(134) Etoc, F.; Balloul, E.; Vicario, C.; Normanno, D.; Lisse, D.; Sittner, A.; Piehler, J.; Dahan, M.; Coppey, M. Non-specific interactions govern cytosolic diffusion of nanosized objects in mammalian cells. *Nat. Mater.* **2018**, *17* (8), 740−746.
(135) Dai, X.; Zhu, Z.; Li, Y.; Yang, B.; Xu, J. F.; Dong, Y.; Zhou, X.; Yan, L. T.; Liu, D. "Shutter" Effects Enhance Protein Diffusion in Dynamic and Rigid Molecular Networks. *J. Am. Chem. Soc.* **2022**, *144* (41), 19017−19025.
(136) Regner, B. M.; Vucinic, D.; Domnisoru, C.; Bartol, T. M.; Hetzer, M. W.; Tartakovsky, D. M.; Sejnowski, T. J. Anomalous diffusion of single particles in cytoplasm. *Biophys. J.* **2013**, *104* (8), 1652−1660.
(137) Qian, H.; Sheetz, M. P.; Elson, E. L. Single particle tracking. Analysis of diffusion and flow in two-dimensional systems. *Biophysical journal* **1991**, *60* (4), 910−921.
(138) Tan, X.; Welsher, K. Particle-by-Particle In Situ Characterization of the Protein Corona via Real-Time 3D Single-Particle-Tracking Spectroscopy. *Angew. Chem.* **2021**, *133* (41), 22533−22541.
(139) Shen, H.; Tauzin, L. J.; Baiyasi, R.; Wang, W.; Moringo, N.; Shuang, B.; Landes, C. F. Single particle tracking: from theory to biophysical applications. *Chem. Rev.* **2017**, *117* (11), 7331−7376.
(140) Bauer, S.; Kirschning, C. J.; Häcker, H.; Redecke, V.; Hausmann, S.; Akira, S.; Wagner, H.; Lipford, G. B. Human TLR9 confers responsiveness to bacterial DNA via species-specific CpG motif recognition. *Proc. Natl. Acad. Sci. U. S. A.* **2001**, *98* (16), 9237−9242.

(141) Sun, L.; Wu, J.; Du, F.; Chen, X.; Chen, Z. J. Cyclic GMP-AMP synthase is a cytosolic DNA sensor that activates the type I interferon pathway. *Science* **2013**, *339* (6121), 786−791.
(142) Rathinam, V. A. K.; Jiang, Z.; Waggoner, S. N.; Sharma, S.; Cole, L. E.; Waggoner, L.; Vanaja, S. K.; Monks, B. G.; Ganesan, S.; Latz, E.; et al. The AIM2 inflammasome is essential for host defense against cytosolic bacteria and DNA viruses. *Nature Immunology* **2010**, *11* (5), 395−402.
(143) Kelly, P. M.; Åberg, C.; Polo, E.; O'Connell, A.; Cookman, J.; Fallon, J.; Krpetić, Ž.; Dawson, K. A. Mapping protein binding sites on the biomolecular corona of nanoparticles. *Nat. Nanotechnol* **2015**, *10* (5), 472−479.

https://doi.org/10.1021/jacsau.4c00986
JACS Au 2025, 5, 17−27